Peer-to-Peer Energy Trading under Network Constraints Based on Generalized Fast Dual Ascent

Changsen Feng, *Member, IEEE*, Bomiao Liang, *Member, IEEE*, Zhengmao Li, *Member, IEEE*, Weijia Liu, *Member, IEEE*, Fushuan Wen, *Fellow, IEEE*

1

***Abstract*— The wide deployment of renewable energy resources, combined with a more proactive demand-side management, is inducing a new paradigm in both power system operation and electricity market trading, which especially boosts the emergence of the peer-to-peer (P2P) market. A more flexible local market mechanism is highly desirable in response to fast changes in renewable power generation at the distribution network level. Moreover, large-scale implementation of P2P energy trading inevitably affects the secure and economic operation of the distribution network. This paper presents a new P2P electricity trading framework with distribution network security constraints considered using the generalized fast dual ascent method. First, an event-driven local P2P market framework is presented to facilitate short-term or immediate local energy transactions. Then, the sensitivity analysis of nodal voltage and network loss with respect to nodal power injections is used to evaluate the impacts of P2P transactions on the distribution network, which ensures the secure operation of the distribution system. Thereby, the external operational constraints are internalized, and the cost of P2P energy trading can be appropriately allocated in an endogenous way. Moreover, a generalized fast dual ascent method is employed to implement distributed market-clearing efficiently. Finally, numerical results indicate that the proposed model could guarantee secure operation of the distribution system with P2P energy trading, and the solution method enjoys good convergence performance.**

***Index Terms* —peer-to-peer (P2P) energy trading, event-driven, market clearing, generalized fast dual ascent.**

I. INTRODUCTION

All over the world, the self-consumption of solar power is currently highly encouraged to reduce the investment demand and operational losses of the transmission and distribution network. As an extension to self-consumption, the emerging peer-to-peer (P2P) energy trading enables prosumers to trade energy using local distribution systems, which may relieve the burden on the transmission grid. As a matter of fact, the decentralized P2P energy trading market is becoming a feasible option (e.g., Brooklyn Microgrid [1], Plico [2]) nowadays, thanks to new advances in information and communication technology [3].

The chief purpose of P2P sharing is to change the traditional centralized hierarchical control mode of power systems and allow for the direct communication and supply of energy among ubiquitous distribution-level prosumers with distributed energy resources (DERs) [4]. In terms of the P2P mechanism design, existing P2P energy trading methods can be divided into four groups: 1) auction theory, 2) game theory, 3) constrained optimization, and 4) blockchain. An auction-based model involves a market where several buyers and sellers seek to interact with one another for trading their goods and simultaneously achieve the objectives of balancing local generation and demand [5], [6] as well as improving prosumers' engagement [7]. An auction-based market is usually difficult to model explicitly because of the stochastic bidding behaviors of its participants. Thus, the game theory is invoked to model behaviors and decisions of P2P market participants through coalitional and non-cooperative games. The application of non-cooperative Nash games in P2P trading can be found for encouraging prosumers' participation in the trading[8], increasing economic benefits to individual participants [9], [10], and clearing bilateral contracts with specifying energy trades and prices [11]. On the other hand, a coalitional game-based model [12], [13] usually focuses on fairness in distributing the revenue obtained by forming prosumers as a grand coalition. To further promote market efficiency in all the diversified game-based models, a few constrained optimization techniques have been used to design P2P energy trading schemes. Specifically, the P2P market clearing is usually formulated as a social welfare maximization problem (e.g., [6], [14], [15] and [16]) and is solved with the most popular solution technique, i.e., alternating direction method of multipliers (ADMM), which is adopted to solve the problem as in [9], [10], [15], [17] and [18]. Currently, the blockchain with the inherent decentralization characteristic has profound applications in P2P trading, leading to the establishment of several blockchain-based platforms for P2P energy trading in recent years. A variety of blockchain-based technologies, e.g., smart contract [19], consortium blockchain [20], Hyperledger IBM [21], are invoked to build the P2P energy trading platform which offers secure and transparent energy trading. In the meantime, the P2P matching mechanisms can also be divided into two categories, namely peer-centric (see [11], [14]) and system-centric (see [16], [18] and [21]), according to the degree of decentralization and topology. The system-centric model possesses a supervisory entity that collects and clears the bids and offers submitted by market agents in a centralized manner [18], like

This work is supported by National Natural Science Foundation of China (No. 52107129, No. U1910216).

C. Feng is with College of Information Engineering, Zhejiang University of Technology, Hangzhou 310023, China (e-mail: fcs@zjut.edu.cn)

B. Liang is with the School of Automation and Electrical Engineering, Zhejiang University of Science and Technology, Hangzhou 310023, China (e-mail: bomiao.liang@zust.edu.cn)

Z. Li is with School of Electrical and Electronic Engineering, Nanyang Technological University, 50 Nanyang Avenue, Singapore 639798, Singapore (email: LIZH0049@e.ntu.edu.sg)

W. Liu is with National Renewable Energy Laboratory, Golden, CO 80401, USA (e-mail: weijia.liu@nrel.gov)

F. Wen is with the Hainan Institute, Zhejiang University, Sanya 572000, China, and with the School of Electrical Engineering, Zhejiang University, Hangzhou 310027, China (e-mail: fushuan.wen@gmail.com).

pool-structured wholesale electricity markets. The peer-centric approach, on the other hand, provides more options to consider prosumers' preferences and offers distributed decision-making protocols to preserve agents' privacy [14].

Although the above mentioned P2P energy trading model could work, the large-scale implementation of P2P energy trading inevitably affects the economic and secure operation of the distribution network. In addition, most of the existing studies ignore the critical physical constraints such as the power flow and nodal voltage constraints, which make them not practical for real-world applications. To consider all the network constraints, sensitivity analysis is employed to evaluate the impacts of P2P transactions in [5] and [7], but how to reasonably recover the extra cost associated with the network constraints is not explicitly described. In [9] and [10] the game model in [17] is extended, with network constraints embedded into the energy management model and a Nash bargaining or noncooperative game theory-based P2P transaction model presented respectively; both methods in [9] and [10] could offer solutions that satisfy axioms of symmetry and Pareto optimality. Nonetheless, there exist some scenarios where the P2P transaction players with weak bargaining power would bear extra costs. In this sense, internalizing the binding constraints in an optimal power flow (OPF) model to present the scarce energy supply by extracting local marginal price (LMP) is paramount.

Apart from the physical limits indicated above, the cost allocation associated with P2P energy trading is another research focus. There are broadly two kinds of cost modeling methods: exogenous cost-based allocation and endogenous cost-based allocation model. The former separates the market transaction from the power grid operation and estimates the ex-post P2P transaction cost to be allocated, like the European power pool market. Authors in [22] exogenously allocate the network losses in a microgrid to the discharging battery storage at each node. The work in [18] intends to implement P2P energy transactions under network constraints and use the DC power flow model to estimate network losses. The latter remains nearly untouched in the literature, which is supposed to internalize external physical constraints by including network constraints in an OPF model and the P2P transaction cost are recovered based on the LMP. The work in [4] couples P2P interactions and distribution network operations as well as uses the distribution LMP to compute network usage fees that agents should pay to the distribution network owners. However, the agents' privacy is not considered when solving the OPF problem in a centralized way in [4].

To protect the agents' privacy as well as improve the system scalability, the distributed operation and control schemes have been extensively studied in recent years. In the literature, the Lagrangian relaxation-based method (LR-M) is widely applied. Specifically, the LR-M primarily includes the traditional LR [23], the auxiliary problem principle [24], ADMM [25], and analytical target cascading [26]. Generally, the LR-M algorithm suffers from a low convergence rate and an inconvenient parameter tuning process but fortunately, the duality theory shows that the Lagrangian multiplier update procedures in LR-M can be viewed as ascent steps in the dual space that maximize the Lagrangian function regarding the Lagrange multipliers. Hence, the dual-based method is adopted to approximate the Lagrange multipliers in LR-M using the gradient-like methods or Newton-like methods, which leads to the development of several multiplier update procedures [27]. In the spirit of the Nesterov accelerated method (NAM), the fast dual ascent method is proposed in [28] and [29] where a Lipschitz constant to the dual function is used to quantify the curvature of the quadratic upper bound of the negative dual function. However, the quadratic upper bound with the same curvature in all directions of [28] and [29] could result in slow convergence, especially under ill-conditioned scenarios. The methods in [30] and [31] further generalize the fast dual ascent, which allows for a quadratic upper bound with different curvatures in different directions, and can approximate the dual function with faster convergence.

With all the above, this paper presents a novel decentralized P2P energy trading model under network constraints using the generalized fast dual ascent (Gf-DA) method. In this paper, an event-driven mechanism is adopted to facilitate short-term or immediate local energy transactions. Comparisons among the key features considered in the existing literature against our proposed method are presented in Table I. The main contributions of this paper are listed as follows:

1) The network constraints are included in the market-clearing problem through the voltage and loss sensitivity method, to ensure secure operations of the power distribution system. In this sense, the external operational constraints are internalized, and the endogenous cost of P2P energy trading is reflected by the location marginal price derived from the market-clearing problem.
2) A LR-based solution method is leveraged to clear the market in a distributed manner whereby a negotiation mechanism between the participants and market operator is provided using the LMP and then makes the clearing method applicable for the short-term P2P energy trading market proposed in this paper.
3) The fast dual ascent method is applied to improve the convergence region and rate of the LR-M algorithm by generalizing the Lipschitz constant. A distributed framework is offered, which effectively protects agents' privacy.

TABLE I
COMPARISON OF THE CONSIDERED FACTORS IN P2P ENERGY TRADING MODEL IN THE EXISTING LITERATURE AND THIS PAPER

Refs.	Network constraints	P2P transaction cost allocation	Agents' privacy protects
[4], [21]	✓	✓	×
[5]	✓	×	×
[6], [11], [15], [16], [17], [19]	×	×	✓
[7],[9],[10],[13],[20]	✓	×	✓
[8], [12]	×	×	×
[14], [18], [22]	×	✓	✓
This Paper	✓	✓	✓

The remainder of the paper is organized as follows: Section II introduces an event-driven market architecture for the proposed P2P market. Section III illustrates the problem formulation for the local P2P energy trading and a decentralized approach for the market clearing is provided in Section IV. A fast dual ascent method is explicitly presented then in Section V to accelerate the market clearing. Finally, in Section VI, the performance of the proposed model is evaluated through numerical analyses, and the key findings of the research are also summarized.

II. The Framework of an Event-Driven P2P Market

An event-driven P2P market mechanism is designed at the distribution system level, which is expected to effectively accommodate the fluctuations and uncertainties in renewable generation outputs. Under this framework, three aspects of the market as follows are clarified.

1) Market participants. All the energy entities, including industrial campuses, local energy communities, etc., can choose to participate in the local energy trading market as sellers or buyers according to their energy surplus or deficit. When certain conditions are met, the event driver automatically triggers market opening, clearing, and other operations. It is assumed there exists a neutral market operator who is responsible for market operation and clearing.

2) Market operation rules. Assume that a day is divided into 144 periods with the market cycle as 10 minutes. The clearing result of the current period will be executed in the next period. Prosumers enter the market by sending transaction requests i.e., trading electricity, price information, and trading periods to the event drivers. Once the market is open, the operator will collect the state data of the distribution network and formulate the market-clearing problem. It is cleared in a distributed manner where each iteration becomes a new round of quotations or bids until the iteration converges or the market closes. It is assumed that the distribution network has the communication network responsible for the information exchange among prosumers and market operators.

3) Event-driven rules. This market is event-driven referring to [16], as it is supposed to work as a backup trading platform, which is unnecessary to be opened permanently for the whole year and is affected by local transaction needs and seasonal events, such as high solar irradiance or energy shortages in regional grids. The event driver set the rules based on local weather conditions such as light intensity, wind speed, the number of trading members as well as the trading power in the market during both current and future periods. The proposed actions of the event driver include waiting, partial-clearance, complete-clearance, and so on. A brief introduction of the actions is given as follows:

(1) Waiting: If there are only sellers or buyers in the market, or there are fewer participants and less trading power, the clearing action will not be performed and postpone the market clearance until the next period.

(2) Partial-clearance: If there is a serious imbalance between selling and buying power, only part of the transaction requests will be cleared to lock the instant revenue so far and delay the rest of the market clearance to the next period.

(3) Complete-clearance: Accept all the bids and offers to perform the standard market clearance.

The event-driven rules should be transparent and indiscriminative to every member of the P2P market. The function of the event-driver can be implemented by the blockchain platform [19], i.e., Smart Contract, of which transparency and immutability are of great importance for P2P energy trading. In addition, it is worth noting that it is not our intention to cover every aspect of the aforementioned market model in a single paper. In this paper, we mainly focus on a more accurate and explicit market-clearing model as well as its solution method.

III. Problem Formulation

A. Preliminary

A radial distribution network is considered. Define *i*, *j*, and *k* as the indices of the nodes in the distribution network. Since each node just holds one prosumer, we abuse notations of the indices of nodes and denote *i* and *j* as the indices of prosumers. Consider a distribution network consisting of *N* prosumers who participate in the local P2P energy trading market. Each prosumer can be either a producer or a consumer at a given time instance. For example, it can act as a producer, when it discharges power to the distribution system, and as a consumer, when it charges power from the distribution system. Thus, the set of prosumers $\mathbf{N}$ can be divided into two groups: producers and consumers. Denote $\mathbf{N}_S = \{1, \ldots, N_S\}$ as the set of producers and $\mathbf{N}_b = \{1, \ldots, N_b\}$ the set of consumers. Obviously, $\mathbf{N} = \mathbf{N}_S \cup \mathbf{N}_b$ and $\varnothing = \mathbf{N}_S \cap \mathbf{N}_b$. Note that vector, matrix, and set are shown in bold capital whereas the index, scalar, and element of the set are expressed in italics and lowercase hereinafter.

B. Consumer and Producer Models

The characteristic of the prosumers' behavior in the P2P energy trading market can be modeled by the concept of the utility function. Here, a quadratic utility function is considered which is corresponding to a linear decreasing marginal benefit. For each consumer *j* participating in the P2P transaction, the utility function is stated as follows:

$$U_j(p_j, q_j) = (-\theta_j^p p_j^2 + \beta_j^p p_j) - \theta_j^q (q_j - q_j^{set})^2 \tag{1}$$

where θ_j^p, β_j^p and θ_j^q are the utility function parameters, which are the private information stored by consumers *j*. The first term in (1) is the utility function which represents the personal satisfaction or convenience for electricity usage. The second term is the cost of the injected reactive power, i.e., the cost caused by the derivation from the previous reactive power q_j^{set} in the P2P transaction. Similarly, the cost function of producer *i* is a quadratic convex function, which also includes the costs of active and reactive power:

$$C_i(p_i, q_i) = a_i^p p_i^2 + b_i^p p_i + \theta_i^q (q_i - q_i^{set})^2 \tag{2}$$

where a_i^p, b_i^p and θ_i^q are the cost function parameters for producer *i*. In addition, the consumers and producers should also comply with the local constraints. Thus, for prosumer $i \in \mathbf{N}$, the local constraints can be described as:

$$\underline{p}_i \le p_i \le \overline{p}_i \tag{3}$$

$$\underline{q}_i \le q_i \le \overline{q}_i \tag{4}$$

where $\overline{p}_i$ / $\underline{p}_i$ are the upper/lower active boundary of prosumer *i*. Similarly, $\overline{q}_i$ / $\underline{q}_i$ the upper/lower reactive boundary of prosumer *i*.

C. Voltage Sensitivity Calculation

The injection model of power flow to node *i* is stated as,

$$\dot{S}_i = \dot{V}_i \left(\sum\nolimits_{j \in \mathbf{\Xi}} Y_{ij} \dot{V}_j \right)^* \tag{5}$$

where $\mathbf{\Xi} = \{1, \ldots, N_A\}$ represents the set of nodes of the distribution network. $\dot{S}_i = P_i + \mathbf{j}Q_i$ and $\dot{V}_i$ are the injected

complex power and voltage phasor of node *i*, respectively. Y_{ij} is the (*i*, *j*) element of the admittance matrix. According to Eqn. (5), the voltage sensitivity with respect to power injections can be calculated as follows. For any node $i \in \Xi$, we have

$$\frac{\partial \dot{S}_i}{\partial P_j} = \frac{\partial \dot{V}_i}{\partial P_j}\left(\sum\nolimits_{j\in\Xi} Y_{ij}\dot{V}_j\right)^* + \dot{V}_i \sum\nolimits_{j\in\Xi} Y_{ij}^* \frac{\partial \dot{V}_j^*}{\partial P_j} = \begin{cases} 0 & i \neq j \\ 1 & i = j \end{cases} \tag{6}$$

$$\frac{\partial \dot{S}_i}{\partial Q_j} = \frac{\partial \dot{V}_i}{\partial Q_j}\left(\sum\nolimits_{j\in\Xi} Y_{ij}\dot{V}_j\right)^* + \dot{V}_i \sum\nolimits_{j\in\Xi} Y_{ij}^* \frac{\partial \dot{V}_j^*}{\partial Q_j} = \begin{cases} 0 & i \neq j \\ 1\mathbf{j} & i = j \end{cases} \tag{7}$$

Obviously, Eqn. (6) is linear with respect to $\partial \dot{V}_i / \partial P_j$ and $\partial \dot{V}_i^* / \partial P_j$, and Eqn. (7) is linear with respect to $\partial \dot{V}_i / \partial Q_j$ and $\partial \dot{V}_i / \partial Q_j$. Hence, voltage sensitivity can be easily obtained by solving the above linear equations. The derivatives of the voltage magnitude with respect to the active/reactive power injections can be calculated as follows. For the *i*-th node,

$$V_i^2 = \dot{V}_i \dot{V}_i^* \Rightarrow 2V_i \frac{\partial V_i}{\partial P_j} = \dot{V}_i \frac{\partial \dot{V}_i^*}{\partial P_j} + \dot{V}_i^* \frac{\partial \dot{V}_i}{\partial P_j} \tag{8}$$

where V_i represents the voltage magnitude of node *i*. Note that the two terms on the right hand of Equation (8) are the conjugate of each other. As the derivative of the magnitude is a real number, the imaginary components must cancel each other out and hence

$$\frac{\partial V_i}{\partial P_j} = \frac{1}{V_i}\mathrm{Re}\left(\dot{V}_i \frac{\partial \dot{V}_i^*}{\partial P_j}\right) \tag{9}$$

The sensitivity of voltage magnitude with respect to reactive power injection can be calculated similarly and can be formulated as

$$\frac{\partial V_i}{\partial Q_j} = \frac{1}{V_i}\mathrm{Re}\left(\dot{V}_i \frac{\partial \dot{V}_i^*}{\partial Q_j}\right) \tag{10}$$

The voltage perturbations caused by the P2P energy trading can then be estimated by employing (8) and (9), which can be stated as:

$$\Delta V(\mathbf{p}, \mathbf{q}) \approx \mathbf{D}_{\mathrm{P}}^{\mathrm{V}}\mathbf{p} + \mathbf{D}_{\mathrm{Q}}^{\mathrm{V}}\mathbf{q} \tag{11}$$

where $\mathbf{p}$ and $\mathbf{q}$ respectively represent the vector of injected active and reactive power of the prosumers in the P2P energy trading market. $\mathbf{D}_{\mathrm{P}}^{\mathrm{V}}$ and $\mathbf{D}_{\mathrm{Q}}^{\mathrm{V}}$ are voltage sensitivity matrices, i.e., $\mathbf{D}_{\mathrm{P}}^{\mathrm{V}}(i, j) = \frac{\partial V_i}{\partial P_j}$ and $\mathbf{D}_{\mathrm{Q}}^{\mathrm{V}}(i, j) = \frac{\partial V_i}{\partial Q_j}$.

D. Loss Sensitivity Calculation

The distribution system structure is assumed to be radial when calculating loss factors in this work. Therefore, the distribution system is of a tree structure, with the distribution substation node as the root of the tree. To facilitate the presentation, nodes and branches are numbered based on the following rules [32]:

1) The index of a node must be greater than the counterparts of its parents.

2) The root is numbered as 1 and all nodes are numbered from 1 to N_A.

3) The branch connecting to a child node *i* is numbered as L_{i-1} and thus the index of branches is from 1 to N_A-1.

$$B(i, j) = \begin{cases} 1 & \text{,if bus } j \text{ belongs to sub-tree of node } i \\ 0 & \text{,otherwise} \end{cases} \tag{12}$$

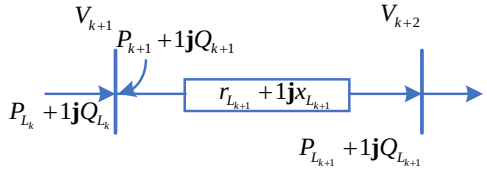

Fig. 1. Single-line diagram of the branch L_{k+1}

Define the line power flow from a parent node to a child node as positive. The line power flow L_k, as shown in Fig. 1, can be calculated by (13) and (14).

$$P_{L_k} = -\sum_{j=k+1}^{N_A} B(k+1, j)\cdot P_j + \sum_{j=k+2}^{N_A} B(k+1, j)\cdot P_{Loss}^{L_{j-1}} \tag{13}$$

$$Q_{L_k} = -\sum_{j=k+1}^{N_A} B(k+1, j)\cdot Q_j + \sum_{j=k+2}^{N_A} B(k+1, j)\cdot Q_{Loss}^{L_{j-1}} \tag{14}$$

In addition, the losses over the line L_k can be attained as

$$P_{Loss}^{L_k} = \frac{P_{L_k}^2 + Q_{L_k}^2}{V_{k+1}^2}\cdot r_{L_k} \tag{15}$$

$$Q_{Loss}^{L_k} = \frac{P_{L_k}^2 + Q_{L_k}^2}{V_{k+1}^2}\cdot x_{L_k} \tag{16}$$

It is assumed that the nodal voltage magnitudes across the distribution network remain unchanged during a slight load change at node *i*. Taking the partial derivatives of both sides of (15)-(16) with respect to power injections, the loss factor of line *k* with respect to the load at node *i* can be attained as:

$$\frac{\partial P_{Loss}^{L_k}}{\partial P_i} = \left(2P_{L_k}\frac{\partial P_{L_k}}{\partial P_i} + 2Q_{L_k}\frac{\partial Q_{L_k}}{\partial P_i}\right)\cdot\frac{r_{L_k}}{V_{k+1}^2} \tag{17}$$

$$\frac{\partial P_{Loss}^{L_k}}{\partial Q_i} = \left(2P_{L_k}\frac{\partial P_{L_k}}{\partial Q_i} + 2Q_{L_k}\frac{\partial Q_{L_k}}{\partial Q_i}\right)\cdot\frac{r_{L_k}}{V_{k+1}^2} \tag{18}$$

$$\frac{\partial Q_{Loss}^{L_k}}{\partial P_i} = \left(2P_{L_k}\frac{\partial P_{L_k}}{\partial P_i} + 2Q_{L_k}\frac{\partial Q_{L_k}}{\partial P_i}\right)\cdot\frac{x_{L_k}}{V_{k+1}^2} \tag{19}$$

$$\frac{\partial Q_{Loss}^{L_k}}{\partial Q_i} = \left(2P_{L_k}\frac{\partial P_{L_k}}{\partial Q_i} + 2Q_{L_k}\frac{\partial Q_{L_k}}{\partial Q_i}\right)\cdot\frac{x_{L_k}}{V_{k+1}^2} \tag{20}$$

Taking the partial derivatives of both sides of (13)-(14) with respect to active and reactive power injections respectively, the load shift factors in (17)-(20) can be substituted and the linear equations with respect to loss factors then obtained. For example, the loss factor of line k with respect to the load at node *i* can be attained by:

$$\frac{\partial P_{Loss}^{L_k}}{\partial P_i} = \frac{2r_{L_k}}{V_{k+1}^2}\cdot\left(-P_{L_k}\cdot B(k+1, j) + \sum_{j=k+2}^{N_A} B(k+1, j)\frac{\partial P_{Loss}^{L_{k-1}}}{\partial P_i}\right) + \frac{2r_{L_k}}{V_{k+1}^2}\cdot\left(-Q_{L_k}\sum_{j=k+2}^{N_A} B(k+1, j)\frac{\partial Q_{Loss}^{L_{k-1}}}{\partial P_i}\right) \tag{21}$$

The loss sensitivity vectors can be obtained by solving the above linear equations. Defining the partial derivatives of the total loss with respect to the bus generation as the summation of the loss factors of each line, and taking the derivatives of

active power loss with respect to the active injection as an example, we can attain

$$\mathbf{D}_{\mathrm{P}}^{\mathrm{P}}=\sum_{L_k=1}^{N_A-1}\frac{\partial P_{Loss}^{L_k}}{\partial P_i} \tag{22}$$

Thereby, the active and reactive losses, i.e., P^{Loss} and Q^{Loss}, can be approximately formulated as:

$$P^{Loss}\approx\mathbf{D}_{\mathrm{P}}^{\mathrm{P}}\cdot\mathbf{p}+\mathbf{D}_{\mathrm{Q}}^{\mathrm{P}}\cdot\mathbf{q} \tag{23}$$

$$Q^{Loss}\approx\mathbf{D}_{\mathrm{P}}^{\mathrm{Q}}\cdot\mathbf{p}+\mathbf{D}_{\mathrm{Q}}^{\mathrm{Q}}\cdot\mathbf{q} \tag{24}$$

where $\mathbf{D}_{\mathrm{Q}}^{\mathrm{P}}$ is the vector consisting of derivatives of active power loss with respect to the reactive power injection. $\mathbf{D}_{\mathrm{P}}^{\mathrm{Q}}$ and $\mathbf{D}_{\mathrm{Q}}^{\mathrm{Q}}$ are the vectors consisting of derivatives of reactive power loss with respect to active and reactive injections, respectively

E. Optimization Model for P2P Energy Trading Market

The P2P energy trading for the distribution network is formulated as a social welfare maximization problem as follows:

$$\min_{\mathbf{p},\mathbf{q}\in\Omega}\left[\sum\nolimits_i C_i(\mathbf{p},\mathbf{q})-\sum\nolimits_i U_i(\mathbf{p},\mathbf{q})\right] \tag{25a}$$

where Ω is the feasibility region of the injected active and reactive power, i.e., $\mathbf{p}$ and $\mathbf{q}$.

A local energy transaction will be physically fulfilled by leveraging the existing distribution lines and smart meters. In the meantime, the impacts caused by P2P transactions should be considered in the optimization model, namely the voltage magnitude constraints along with the power balance constraints.

$$\underline{\mathbf{V}}\le\hat{\mathbf{V}}+\Delta\mathbf{V}(\mathbf{p},\mathbf{q})\le\bar{\mathbf{V}}\ \ (\boldsymbol{\mu}_{\max},\boldsymbol{\mu}_{\min}) \tag{25b}$$

$$\sum\nolimits_i p_i-P^{Loss}(p,q)=0\quad(\lambda_p) \tag{25c}$$

$$\sum\nolimits_i q_i-Q^{Loss}(p,q)=0\quad(\lambda_q) \tag{25d}$$

where $\hat{\mathbf{V}}$ is the vector of nodal voltage before implementing the P2P transactions. Eqn. (25b) imposes voltage magnitude limit on each node, where $\underline{\mathbf{V}}$ and $\bar{\mathbf{V}}$ are the vector of lower and upper limits of nodal voltage magnitude, respectively. $\boldsymbol{\mu}_{\max}$ and $\boldsymbol{\mu}_{\min}$ are the Lagrangian multipliers associated with voltage limits. Eqns. (25c) and (25d) respectively indicate the active and reactive power balances with which the Lagrangian multipliers, i.e., λ_p and λ_q, are associated.

IV. Mechanism Design of Market Clearing

The market-clearing problem in (25) can be solved in a centralized manner with a coordinator collecting all the information of prosumers. However, this will inevitably violate the privacy of agents, which is undesirable and unreasonable in a P2P market. Hence, a LR-based distributed solution method, referred to as LR-DM, is proposed to solve (25), where each agent solves its sub-problem locally with limited information exchange with the market operator. Due to the presence of spatially coupled constraints (25b), (25c), and (25d), problem (25) is decomposed into a series of sub-problem which can be solved in a distributed way. Here, we intend to excavate the specific meaning of LR-DM and take LMP as the crucial information to coordinate the prosumers.

At first, the Lagrangian function is given as (26).

$$\begin{aligned}\ell(\mathbf{p},\mathbf{q},\boldsymbol{\mu}_{\max},\boldsymbol{\mu}_{\min},\lambda_p,\lambda_q)=&\sum\nolimits_{i\in N_b}U_i(p_i,q_i)-\sum\nolimits_{j\in N_s}C_j(p_j,q_j)\\&+\boldsymbol{\mu}_{\max}^{\mathrm{T}}\cdot\left(\hat{\mathbf{V}}+\Delta\mathbf{V}(\mathbf{p},\mathbf{q})-\bar{\mathbf{V}}\right)\\&+\boldsymbol{\mu}_{\min}^{\mathrm{T}}\cdot\left(\underline{\mathbf{V}}-\hat{\mathbf{V}}-\Delta\mathbf{V}(\mathbf{p},\mathbf{q})\right)\\&+\lambda_p\cdot\left(\sum\nolimits_{i\in N_b}p_i-\sum\nolimits_{j\in N_S}p_j-P^{Loss}(\mathbf{p},\mathbf{q})\right)\\&+\lambda_q\cdot\left(\sum\nolimits_{i\in N_b}q_i-\sum\nolimits_{j\in N_S}q_j-Q^{Loss}(\mathbf{p},\mathbf{q})\right)\end{aligned} \tag{26}$$

Assuming that the multipliers can be accurately estimated, then, the Lagrangian function can be solved in a distributed manner based on the principle of dual decomposition. For example, the prosumers solve their local problems after receiving the multipliers in the t^{th} iteration:

$$\{p_n^{(t)},q_n^{(t)}\}:=\arg\min_{p_n,q_n\in\Omega}\ell(\mathbf{p},\mathbf{q},\boldsymbol{\mu}_{\max}^{(t)},\boldsymbol{\mu}_{\max}^{(t)},\lambda_p^{(t)},\lambda_q^{(t)}) \tag{27}$$

In the iteration procedures, the multipliers should be updated to guarantee the convergence to the optimum values of the primal problem. The sub-gradient method is used to update the values of multipliers, which is stated as:

$$\lambda_p{}^{t+1}=[\lambda_p{}^{t}-\kappa\nabla_{\lambda_p}\ell] \tag{28a}$$

$$\lambda_q{}^{t+1}=[\lambda_q{}^{t}-\kappa\nabla_{\lambda_q}\ell] \tag{28b}$$

$$\boldsymbol{\mu}_{\max}^{t+1}=[\boldsymbol{\mu}_{\max}^{t}-\kappa\nabla_{\boldsymbol{\mu}_{\max}}\ell]^{+} \tag{28c}$$

$$\boldsymbol{\mu}_{\min}^{t+1}=[\boldsymbol{\mu}_{\min}^{t}-\kappa\nabla_{\boldsymbol{\mu}_{\min}}\ell]^{+} \tag{28d}$$

where κ is the step size. Obviously, (27) and (28) are explicable only in the sense of mathematics. Next, we intend to excavate the specific meanings of (27) and (28), which makes the above-distributed algorithm applicable in P2P electricity market clearing. At first, we define the LMP for the active and reactive power [33], [34] as follows:

$$\begin{cases}\tau_p^{(t)}=\lambda_p^{(t)}\cdot\left(\mathbf{D}_{\mathrm{P}}^{\mathrm{P}}-1\right)+\lambda_q^{(t)}\cdot\mathbf{D}_{\mathrm{P}}^{\mathrm{Q}}\cdot-\boldsymbol{\mu}_{\max}^{(t)}\cdot\mathbf{D}_{\mathrm{P}}^{\mathrm{V}}+\boldsymbol{\mu}_{\min}^{(t)}\cdot\mathbf{D}_{\mathrm{P}}^{\mathrm{V}}\\ \tau_q^{(t)}=\lambda_p^{(t)}\cdot\mathbf{D}_{\mathrm{Q}}^{\mathrm{P}}+\lambda_q^{(t)}\cdot\left(\mathbf{D}_{\mathrm{Q}}^{\mathrm{Q}}-1\right)-\boldsymbol{\mu}_{\max}^{(t)}\cdot\mathbf{D}_{\mathrm{Q}}^{\mathrm{V}}+\boldsymbol{\mu}_{\min}^{(t)}\cdot\mathbf{D}_{\mathrm{Q}}^{\mathrm{V}}\end{cases} \tag{29}$$

Then, (27) can be seen as the prosumer n locally solving the following problem as (29) with the objective function of maximizing its total revenue (i.e., utility function minus the cost of purchasing active and reactive power).

$$\{p_n^{(t)},q_n^{(t)}\}:=\arg\min_{p_n,q_n\in\Omega}-U_n(p_n,q_n)+\tau_{p,n}^{(t-1)}p_n+\tau_{q,n}^{(t-1)}q_n \tag{30}$$

The prosumer n solves its problem and then submits the bid or offer of active and reactive power to the market operator. According to the received bids and offers from prosumers, the market operator calculates the LMPs, as shown in (28) and (29), and broadcasts them to prosumers in the P2P energy trading market as the iteration continues.

V. Generalized Fast Dual Ascent Methodologies

The traditional LR-DM needs to tune the step size for better convergence performance. Sometimes it may even suffer from poor convergence if the dual is ill-conditioned. Here, we use the fast dual ascent method to improve and accelerate the convergence performance. For ease of the presentation hereafter, the optimization model (25) is compactly formulated as (31).

$$\begin{cases} \min\limits_{\mathbf{p},\mathbf{q}\in\Omega} f(\mathbf{p},\mathbf{q}) \coloneqq \frac{1}{2}\left\|\mathbf{p}-\mathbf{p}_r\right\|_{\mathbf{H_P}}^2 + \frac{1}{2}\left\|\mathbf{q}-\mathbf{q}_r\right\|_{\mathbf{H_Q}}^2 \\ \underline{\mathbf{V}} \le \mathbf{D}_{\mathrm{P}}^{\mathrm{V}}\mathbf{p} + \mathbf{D}_{\mathrm{Q}}^{\mathrm{V}}\mathbf{q} \le \bar{\mathbf{V}} \quad \boldsymbol{\mu}_{\max}, \boldsymbol{\mu}_{\min} \\ 1_N\mathbf{p} - \mathbf{D}_{\mathrm{P}}^{\mathrm{P}}\mathbf{p} + \mathbf{D}_{\mathrm{Q}}^{\mathrm{P}}\mathbf{q} = 0 \quad \lambda_p \\ 1_N\mathbf{q} + \mathbf{D}_{\mathrm{P}}^{\mathrm{Q}}\mathbf{p} - \mathbf{D}_{\mathrm{Q}}^{\mathrm{Q}}\mathbf{q} = 0 \quad \lambda_q \end{cases} \tag{31}$$

where matrices $\mathbf{H_P}$, $\mathbf{H_Q}$, $\mathbf{p}_r$ and $\mathbf{q}_r$ are extracted from the utility and cost function as shown in (1) and (2).

A. Fast Dual Ascent Method

First-order optimality conditions for (27) using $\mathbf{p}$ and $\mathbf{q}$ respectively are $\nabla_{\{\mathbf{p},\mathbf{q}\}}\ell = 0$. Hence, the dual function can be described as (32).

$$d(\boldsymbol{\delta}) \coloneqq \inf_{\mathbf{p},\mathbf{q}} \ell = -\frac{1}{2}\boldsymbol{\delta}^T\mathbf{M}\mathbf{H}^{-1}\mathbf{M}^T\boldsymbol{\delta} - (\mathbf{M}\mathbf{H}^{-1}\mathbf{g}+\mathbf{z})^T\boldsymbol{\delta} \tag{32}$$

where

$$\boldsymbol{\delta} \coloneqq \begin{bmatrix} \boldsymbol{\mu}_{\max} \\ \boldsymbol{\mu}_{\min} \\ \lambda_p \\ \lambda_q \end{bmatrix} \quad \mathbf{M} = \begin{bmatrix} \mathbf{D}_{\mathrm{P}}^{\mathrm{V}} & \mathbf{D}_{\mathrm{Q}}^{\mathrm{V}} \\ -\mathbf{D}_{\mathrm{P}}^{\mathrm{V}} & -\mathbf{D}_{\mathrm{Q}}^{\mathrm{V}} \\ 1_N - \mathbf{D}_{\mathrm{P}}^{\mathrm{P}} & \mathbf{D}_{\mathrm{Q}}^{\mathrm{P}} \\ \mathbf{D}_{\mathrm{P}}^{\mathrm{Q}} & 1_N - \mathbf{D}_{\mathrm{Q}}^{\mathrm{Q}} \end{bmatrix} \quad \mathbf{z} \coloneqq \begin{bmatrix} \bar{\mathbf{v}} \\ -\underline{\mathbf{v}} \\ 0 \\ 0 \end{bmatrix}$$

$$\mathbf{H} = \begin{bmatrix} \mathbf{H_P} & \\ & \mathbf{H_Q} \end{bmatrix} \qquad \boldsymbol{\varphi} = \mathbf{H}\begin{bmatrix} -\mathbf{p}_r \\ -\mathbf{q}_r \end{bmatrix}$$

Then, the dual problem can be stated as

$$\max_{\boldsymbol{\mu}_{\max},\boldsymbol{\mu}_{\min}\ge 0,\lambda_p,\lambda_q} d(\boldsymbol{\delta}) \tag{33}$$

Provided that problem (30) is convex with a convex objective function and convex constraints, the dual function d is differentiable, and its gradient can be represented as

$$\nabla d(\boldsymbol{\delta}) = \mathbf{M}\begin{bmatrix} \mathbf{p}^*(\boldsymbol{\delta}) \\ \mathbf{q}^*(\boldsymbol{\delta}) \end{bmatrix} - \mathbf{z} \tag{34}$$

where $\left\{\mathbf{p}^*(\boldsymbol{\delta}), \mathbf{q}^*(\boldsymbol{\delta})\right\} = \arg\min_{\mathbf{p},\mathbf{q}} \ell$.

By (34), for any $\boldsymbol{\delta}^{(1)}$ and $-\boldsymbol{\delta}^{(2)}$, we get

$$\left\|-\nabla d(\boldsymbol{\delta}^{(1)}) + \nabla d(\boldsymbol{\delta}^{(2)})\right\|_2 \le \left\|\mathbf{M}\mathbf{H}^{-1}\mathbf{M}^T\right\|_2 \left\|\boldsymbol{\delta}^{(1)} - \boldsymbol{\delta}^{(2)}\right\|_2 \tag{35}$$

which implies $-d$ has a Lipschitz continuous gradient with constant $L = \left\|\mathbf{M}\mathbf{H}^{-1}\mathbf{M}^T\right\|_2$. Hence, it motivates us to use the fast gradient method to solve the dual problem instead of using a sub-gradient method. The basic idea of the fast gradient method is to maximize the bound in each update instead of directly maximizing d. Hence, the definition of the Lipschitz constant can be generalized to fit a tighter bound with different curvatures in different directions, thus guaranteeing a closer approximation and a faster convergence. Generalize the Lipschitz constant $\left\|\mathbf{M}\mathbf{H}^{-1}\mathbf{M}^T\right\|_2$ to $\mathbf{M}\mathbf{H}^{-1}\mathbf{M}^T$, then for any $\boldsymbol{\delta}^{(1)}$ and $-\boldsymbol{\delta}^{(2)}$, it attains

$$d(\boldsymbol{\delta}^{(1)}) \ge d(\boldsymbol{\delta}^{(2)}) + \nabla d(\boldsymbol{\delta}^{(2)})^{\mathrm{T}}(\boldsymbol{\delta}^{(1)} - \boldsymbol{\delta}^{(2)}) - \frac{1}{2}\left\|\boldsymbol{\delta}^{(1)} - \boldsymbol{\delta}^{(2)}\right\|_{\mathbf{L}}^2 \tag{36}$$

where $\mathbf{L} \succeq \mathbf{M}\mathbf{H}^{-1}\mathbf{M}^T$. Obviously, the $\boldsymbol{L}$-norm term in the right hand of (35) brings a lower bound with which the fast gradient method is used to solve the problem (33), which is referred to as Gf-DA. The updating rule of Gf-DA is presented in Algorithm 1.

Algorithm 1: Generalized fast dual ascent

Initialization: Set $\lambda_p(1) = \lambda_q(1) = 0$, $\boldsymbol{\mu}_{\max}(0) = \boldsymbol{\mu}_{\min}(0) \ge 0$ and $\sigma(1) = 1$.

For $t \ge 1$, update the primal and dual variables by the following steps:

S1: For prosumer n, receive the LMP information and solve the following problem minimizing its total cost:

$$\{p_n^{(t)}, q_n^{(t)}\} \coloneqq \arg\min_{p_n, q_n \in \Omega} -U_n(p_n, q_n) + \tau_{p,n}^{(t-1)} p_n + \tau_{q,n}^{(t-1)} q_n$$

Then, the market operator updates the multipliers and calculates the LMP

S2:
$$\begin{cases} \boldsymbol{\mu}_{\max}^{(t)} = \left[\boldsymbol{\beta}_{\max}^{(t)} + [\mathbf{L}^{-1}]_{\boldsymbol{\beta}_{\min}} * \nabla_{\boldsymbol{\mu}_{\max}} d(\boldsymbol{\gamma}^{(t)})\right]_0^{\infty} \\ \boldsymbol{\mu}_{\min}^{(t)} = \left[\boldsymbol{\beta}_{\min}^{(t)} + [\mathbf{L}^{-1}]_{\boldsymbol{\beta}_{\min}} * \nabla_{\boldsymbol{\mu}_{\min}} d(\boldsymbol{\gamma}^{(t)})\right]_0^{\infty} \\ \lambda_p^{(t)} = \pi_p^{(t)} + [\mathbf{L}^{-1}]_{\pi_p} * \nabla_{\lambda_p} d(\boldsymbol{\gamma}^{(t)}) \\ \lambda_q^{(t)} = \pi_q^{(t)} + [\mathbf{L}^{-1}]_{\pi_q} * \nabla_{\lambda_q} d(\boldsymbol{\gamma}^{(t)}) \end{cases}$$

S3: $\sigma^{(t+1)} = \dfrac{1+\sqrt{1+4\sigma^{(t)2}}}{2}$ and $\upsilon^{(t)} = \dfrac{\sigma^{(t)}-1}{\sigma^{(t)}}$

S4:
$$\begin{cases} \boldsymbol{\beta}_{\max}^{(t+1)} = \boldsymbol{\mu}_{\max}^{(t)} + \upsilon^{(t)}(\boldsymbol{\mu}_{\max}^{(t)} - \boldsymbol{\mu}_{\max}^{(t-1)}) \\ \boldsymbol{\beta}_{\min}^{(t+1)} = \boldsymbol{\mu}_{\min}^{(t)} + \upsilon^{(t)}(\boldsymbol{\mu}_{\min}^{(t)} - \boldsymbol{\mu}_{\min}^{(t-1)}) \\ \pi_p^{(t+1)} = \lambda_p^{(t)} + \upsilon^{(t)}(\lambda_p^{(t)} - \lambda_p^{(t-1)}) \\ \pi_q^{(t+1)} = \lambda_q^{(t)} + \upsilon^{(t)}(\lambda_q^{(t)} - \lambda_q^{(t-1)}) \end{cases}$$

S5: Calculate the LMP as stated in (29).

where $[\bullet]_a^b$ denotes the projection operation onto the set [a, b]; $[\mathbf{L}^{-1}]_{\boldsymbol{\mu}_{\max}}$, $[\mathbf{L}^{-1}]_{\boldsymbol{\mu}_{\min}}$, $[\mathbf{L}^{-1}]_{\lambda_p}$ and $[\mathbf{L}^{-1}]_{\lambda_q}$ are the submatrices of $\mathbf{L}^{-1}$ consisting of the rows with respect to the dual variables denoted by the subscript.

B. Convergence Analysis

First, we will discuss the prerequisite which guarantees the convergence of LR-DM and the Df-GA for solving the proposed model. To ensure the convergence of LR-DM, the step size κ in (28) should be sufficiently small such that $0 \le \kappa \le 2/L$ where L is the Lipschitz constant in (35) and $L = \left\|\mathbf{M}\mathbf{H}^{-1}\mathbf{M}^T\right\|_2$. It can be proved by using the descent lemma and readers can refer to [27] for more details. As for the generalized fast dual ascent, we can set $\mathbf{L} \succeq \mathbf{M}\mathbf{H}^{-1}\mathbf{M}^T$ so that a quadratic upper bound of the dual function is obtained and thus guarantee the convergence when solving the dual problem.

Next, the convergence rates of the LR-DM and Gf-DA will be compared. Denote the optimum of primal and dual problems as $\{\mathbf{p}^*, \mathbf{q}^*\}$ and $\boldsymbol{\delta}^*$, respectively. The initial gaps are defined as

$$C_2 = \left\|\boldsymbol{\delta}^{(0)} - \boldsymbol{\delta}^*\right\|_2^2 \text{ and } C_{\mathbf{L}} = \left\|\boldsymbol{\delta}^{(0)} - \boldsymbol{\delta}^*\right\|_{\mathbf{L}}^2 \tag{37}$$

Then, we get the following lemma:

Lemma-1: Suppose that both the step size κ in the LR-DM and matrix $\mathbf{L}$ in the Gf-DA are set appropriately to guarantee the convergence, it yields:

$$d(\boldsymbol{\delta}^*) - d(\boldsymbol{\delta}^{(t)}) \le \frac{C_2}{2\kappa t} \text{ and } d(\boldsymbol{\delta}^*) - d(\boldsymbol{\delta}^{(t)}) \le \frac{2C_{\mathbf{L}}}{(t+1)^2} \quad (38)$$

Proof: The first part can be easily proved by the descent lemma (see [27] for details). The second part can be seen in the appendix.

From Lemma 1, it can be concluded that Gf-DA solves the problem with a convergence rate no worse than $O(1/t^2)$ whereas the LR-DM only achieves a rate of $O(1/t)$. It shows that the proposed method could significantly improve the convergence of LR-DM for the organization of an event-driven P2P energy trading market.

C. How to Choose L?

Picking a proper step size is critical and difficult in the LR-DM while it is unnecessary to empirically tune the step size in Gf-DA since the dual multipliers can be updated in different directions represented by the matrix **L**. Therefore, the main task in the implementation is how to determine the matrix **L**. According to (34), $\mathbf{L} = \mathbf{M}\mathbf{H}^{-1}\mathbf{M}^T$ provides the tightest bound which thus offers the fastest convergence. However, **M** is obviously not a row full rank matrix, which makes **L** not invertible. To deal with the dilemma, we first assume **L** is a diagonal matrix, though it may slow the convergence to a certain degree. Then, **L** can be obtained by solving a semi-definite programming problem as follows:

$$\begin{cases} \min\limits_{\mathbf{L}} \text{Trace}(\mathbf{L}) \\ \mathbf{L} \succeq \mathbf{M}\mathbf{H}^{-1}\mathbf{M}^T \end{cases} \quad (39)$$

There is another concern that should be addressed, i.e., how to get the **H** matrix. The matrix **H** consists of the economic parameters of the prosumers, to which the neutral market operator or coordinator has no access due to privacy concerns and market fairness. Two cases are considered here, one with a market operator who can estimate the values in the **H** matrix using the information in the bids/offers in the successive two iterations [31], the other with no market operator or coordinator, whose matrix **L** is computed in a distributed way based on the distributed version of the generalized Lipschitz condition [30].

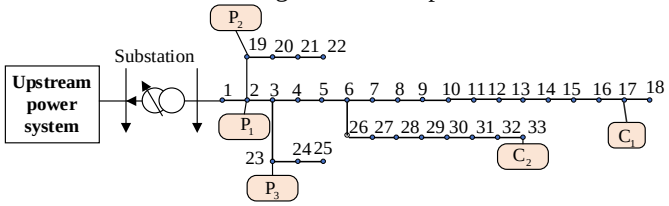

Fig. 2. IEEE 33-bus distribution network with five prosumers

VI. Case Studies

All numerical experiments are conducted in MATLAB R2014a on a laptop with an Intel Core (i7, 2.80GHz) and 16GB memory.

A. System Setting

In this paper, a modified 33-bus test system is employed to demonstrate and analyze the proposed local P2P power trading market, as shown in Fig. 2. Suppose 5 prosumers are participating in the market, located at nodes 2, 17, 19, 23, 33. Among them, prosumers at nodes 17 and 33 are consumers (denoted as C_1 and C_2), whereas those at the rest three nodes are producers (denoted as P_1, P_2, and P_3, successively). It should be noted that all distribution network nodes have the basic load, adopting the same value as those in the original test system. The step size κ and the initial value in the Lagrange multiplier in LR-DM are set to 0.001 and 0, respectively. The lower and upper limits of nodal voltage magnitude are set as 0.91 and 1.09, respectively. In addition, the L-∞ norm is used to define the stopping criterion for checking convergence. Denote the vector Φ as the LMPs for active and reactive power, then

$$\left\| \Phi^{(t)} - \Phi^{(t-1)} \right\|_\infty \le 10^{-4} \quad (40)$$

Eqn. (40) means that the iteration process continues until the largest deviation of LMPs in the two successive iterations is smaller than 10^{-4}.

The utility function, cost function coefficient, and upper and lower limits of output constraints of community operators are taken from the ref. [14]. Referring to [32], assume the coefficients of reactive power cost function as 1/10 of those of active power cost function, as shown in Table II.

TABLE II
THE BASIC PARAMETERS OF PROSUMERS

Consumer	θ_i^p ($/kWh^2)	β_i^p ($/kWh)	θ_i^q ($/kVarh^2)	$\overline{p}_i$ (kW)	$\underline{p}_i$ (kW)	$\overline{q}_i$ (kVar)	$\underline{q}_i$ (kVar)
C_1	0.0080	0.625	0.0008	20	0	10	-10
C_2	0.0090	0.590	0.0009	25	0	15	-15
Producer	a_j^p ($/kWh^2)	b_j^p ($/kWh)	θ_i^q ($/kVarh^2)	$\overline{p}_j$ (kW)	$\underline{p}_j$ (kW)	$\overline{q}_j$ (kVar)	$\underline{q}_j$ (kVar)
P_1	0.0040	0.205	0.0008	30	0	30	-30
P_2	0.0030	0.330	0.0006	20	0	20	-20
P_3	0.0035	0.330	0.0007	20	0	20	-20

B. Sensitivity Analysis

In this section, the sensitivity and error of voltage and network loss are analyzed [32]. Five nodes are first selected arbitrarily in the test system (nodes 5, 6, 15, 16, and 28 in this case), and then a certain amount of active power and reactive power are injected into the selected nodes. The injected power to each node follows the normal distribution, as shown in (41).

$$\Delta_i \sim N(0,\ 0.15 \times \Lambda_i) \quad (41)$$

where Δ_i is the active or reactive power injected into node i and Λ_i is the baseload power of node i.

The Newton-Raphson method and the sensitivity model presented in this paper are used to calculate the voltage amplitude of each node and network loss in the distribution network, respectively. The results from the Newton-Raphson method are calculated with the Matpower 7.0 and are taken as the benchmark. It can be found from Table III that the error of voltage amplitude and network loss obtained by the sensitivity method proposed in this paper are controlled within 1 ‰ and 3%, both of which have high accuracy.

TABLE III
ERROR ANALYSIS OF VOLTAGE AND LOSS SENSITIVITY MODEL

No.	1	2	3	4	5
maximum error of nodal voltage magnitude (%)	0.07	0.08	0.06	0.07	0.07
error of network loss (%)	0.29	2.96	0.08	1.88	2.33

C. Performance Analysis

To analyze the impact of the P2P power trading market on the operations of the distribution network, the following three modes are set up for comparative analysis:

Mode 1: A P2P electricity trading market without considering voltage constraints.

Mode 2: A P2P electricity trading market without considering network loss.

Mode 3: A P2P electricity trading market considering both voltage constraints and network loss as proposed in this paper.

It can be observed that without considering voltage constraints, i.e., mode 1, the nodal voltage amplitude of the end node, i.e., node 18 in the test system, drops to 0.9090 during P2P power trading, which obviously violates the lower limit. In mode 3, the injected reactive power in C_1 and C_2 increases compared to mode 1, effectively reducing the voltage drop of the feeder and thereby avoiding violating voltage constraints. When the network loss is not considered (mode 2), the trading power of each market agent fluctuates slightly.

TABLE IV
OPERATIONAL DATA IN MODES 1, 2 AND 3

Mode	Injected power	P_1	P_2	P_3	C_1	C_2	voltage at node 18
1	Active(kW)	23	9.8	10	-22.8	-17.2	0.908
	Reactive(kVar)	-9.4	-12.3	-1.2	15	10	
2	Active(kW)	20.6	6.6	6.7	-12.8	-21.1	0.910
	Reactive(kVar)	-8.7	-11.5	-4.8	15	10	
3	Active(kW)	20.2	6.2	7.3	-14.1	-17.9	0.910
	Reactive(kVar)	-10.4	-13.6	0.3	15	10	

Note: Define the injection power as the positive value

TABLE V
LOCATIONAL MARGINAL PRICE IN MODES 2 AND 3

	Electricity price	P_1	P_2	P_3	C_1	C_2
Mode 2	Active($/kWh)	0.3697	0.3697	0.3766	0.5229	0.4002
	Reactive($/kVarh)	-0.0069	-0.0069	-0.0034	0.1205	0.0136
Mode 3	Active ($/kWh)	0.3667	0.3669	0.3812	0.5122	0.4292
	Reactive ($/kVarh)	-0.0083	-0.0082	-0.0002	0.1001	0.0403

Note: The electricity prices in the above are selling prices.

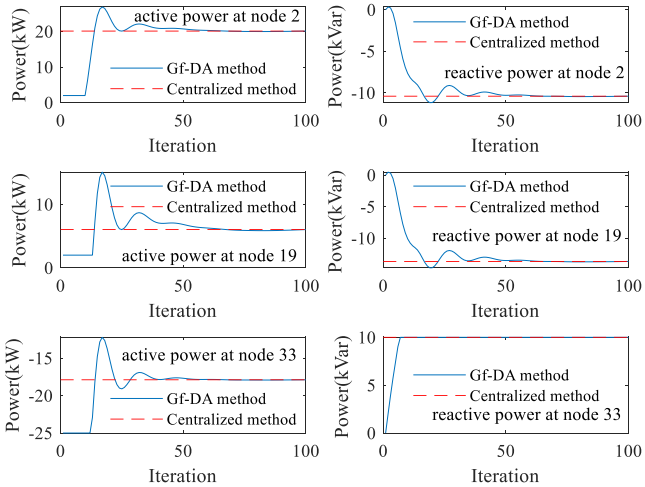

Fig.3 The iteration process of selected nodes (i.e., nodes 2, 19, and 33) in mode3 using the Gf-DA method

It can be found in Table V that the price of active power nearly remains constant for each prosumer in mode 2. This is because the LMP mechanism partly degenerated into the uniform pricing mechanism when the network loss is neglected. The LMP mechanism for the reactive power still works as the voltage drops at the end node can be mitigated by dispatching the reactive power of each prosumer at a relatively low cost.

As shown in Table V, the LMP information could effectively present the scarcity of the active and reactive power for each node in mode 3. Note that prices for the reactive power at different nodes are positive or negative values. For example, the reactive power price for P_1 is negative, indicating that excess reactive power needs to be absorbed in the corresponding node. Combining with Table IV, we can get that each prosumer obtains a positive benefit by generating or absorbing reactive power. This is reasonable because it will bring the certain cost to be recovered regardless of generating or absorbing reactive power for the prosumers, which is also consistent with the modeling of reactive power cost in (1) and (2). It also can be obtained that the LMP approach penalizes users who contribute to distribution bottlenecks and rewards users who tend to alleviate them. In addition, the merchandise surplus brought by the network loss and voltage constraints guarantees the revenue adequacy in the proposed P2P energy market, which can also be verified by Tables IV and V.

The iteration process of the trading active and reactive power of selected market agents in mode 3 is shown in Fig. 3 while the iteration process of λ_q is depicted in Fig. 4. As shown in Fig. 3, each market agent could reach convergence in 51 iterations, which makes the proposed Df-GA applicable in the short-term P2P energy trading market proposed in this paper.

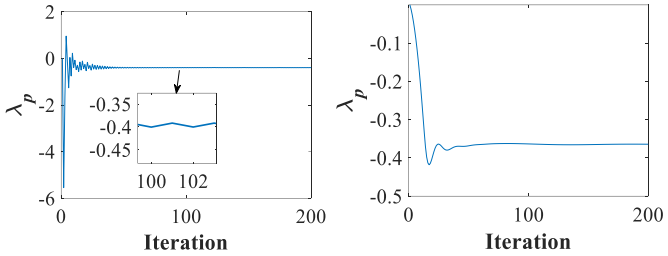

Fig.4 Iteration process of λ_q: (a) LR-DM; (b) Gf-DA.

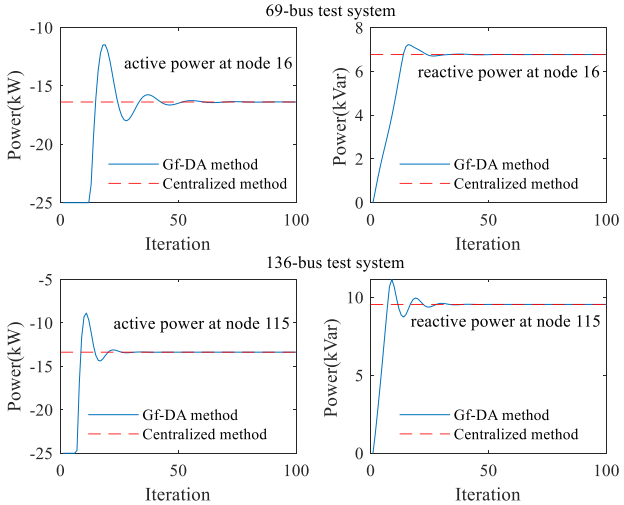

Fig.4 The iteration process of selected nodes in the 69-bus and 136-bus test systems

D. Comparison Between LR-DM and Gf-DA

It can be found in Fig. 4 that Gf-DA can converge in 51 iterations while the LR-DM could not converge even in 200 iterations. This is mainly because the constraint of voltage magnitude limit on node 18 is binding in mode 3 so that the LR-DM could not find a feasible solution and even oscillate around the optimum. In addition, the Gf-DA method converges to the optimum values monotonically in the first 10 iterations while

the LR-DM arouses zigzagging and abrupt changes. It is reasonable because the Gf-DA updates the multipliers in different directions while the sub-gradient method mainly focuses on improving performance per iteration. Note that there respectively exist closed-form solutions to the primal and dual problems in Gf-GA, which enables it to avoid solving the optimization problem in each update. Thus, the solution time for Gf-DA is merely 0.1862s which is too short to be neglected in a P2P market cycle.

E. Scalability Analysis

Two test systems, i.e., the 69-bus with 28 prosumers and the 136-bus with 52 prosumers, are used to demonstrate the scalability of the proposed technique. The nodes associated with the prosumers are shown in Table VI and the remaining parameters for the prosumers are the same as those in Table II. Besides, the step-size scheme in mode 3 is still used in this study. The results of this study are provided in Table VI and Fig.4 is employed to depict the iteration process of the trading active and reactive power of selected market agents. As is shown in Table VI and Fig.4, Gf-DA can achieve convergence at a relatively high speed regardless of the scale of the test system or the number of prosumers. This is reasonable because the time required to implement the five steps in Gf-DA is negligibly short since a closed solution can be derived in the S2 and simple algebraic operations are conducted in S3, S4, and S5. Besides, the iteration number for LR-DM with respect to the two test systems is much higher than those of Gf-DA and so does the computation time. Hence the proposed method enjoys a better convergence performance.

TABLE VI
COMPARISONS OF SCALABILITY PERFORMANCE FOR GF-DA AND LR-DM

Systems	Prosumers	Gf-DA		LR-DM	
		Iteration	Time/s	Iteration	Time/s
69-bus with 28 prosumers	**Producers:** {2 9 12 15 22 24 32 36 40 41 57 59 66 67}; **Consumers:** {5 8 16 18 25 27 35 39 43 47 50 52 61 64};	47	0.762	809	31.69
136-bus with 52 prosumers	**Producers:** {2 5 11 12 22 26 31 33 42 45 51 53 62 65 74 77 81 85 91 101 117 132}; **Consumers:** {3 8 17 19 23 26 38 47 49 54 56 62 68 73 79 86 88 96 98 106 109 115 116 125 128 131 133};	35	1.319	1731	154.0

F. Robust Performance Analysis

The packet dropout during the information exchange is unpredictable, which can be modeled as a stochastic process known as burst noise [35]. Besides, the communication delay can also be modeled as a probability model, which determines the data packet delivery rate[36]. Here, we take the packet dropout as an example to study the robustness of the proposed solution method. A Gilbert-Elliott model is invoked to model the packet dropout process. Two states, i.e., the good (G) and the bad (B) are considered in this model, each of which may generate errors as independent events with the state-dependent error rates, 1- ω_1 (good) and 1- ω_2 (bad), respectively. The transition probabilities between the states are defined by, ρ_1: G-state to B-state, ρ_2: B-state to G-state. The stationary state probabilities ρ_G and ρ_B exist for $0 < \rho_1, \rho_2 < 1$, which can be respectively stated as

$$\rho_G = \rho_2 / (\rho_1 + \rho_2) \text{ and } \rho_B = \rho_1 / (\rho_1 + \rho_2) \quad (42)$$

Thereby, the error rate ρ_E of the transmission channel can be obtained in the stationary state as:

$$\rho_E = (1-\omega_1)\rho_G + (1-\omega_2)\rho_B \quad (43)$$

The values of $\rho_1 = 0.00253$ and $\rho_2 = 0.25$ are used for all cases [37]. As mentioned in [35], the value of ω_2 is selected around 0.5, and ω_1 can be calculated to attain the desired dropout rate. Thus, the values of ω_2=0.5 along with ω_1=0.995, 0.955 0.904 and 0.80 are chosen for the packet dropout rate ρ_E 1%, 5%, 10% and 20%, respectively.

Here it is assumed that the dropout rates of both market operator and peers are set as the values of ρ_E. Specifically, if the market operator does not receive information from the peers and vice versa, they simply use the information in the previous iteration as the interaction process continues. As shown in Table VII, the solution method can converge to the optimum when facing the random packet dropout and more iterations will be demanded with a higher probability of communication failure. Compared with the perfect communication mode, i.e., $\rho_E = 0$, the iteration number does not change remarkably regardless of IEEE 33-bus, 69-bus, or 136-bus test systems when the packet dropout rate is smaller than 0.1. Even when the dropout rate is 0.2 which is rare in the practical scenarios, the solution method still could converge in a permissible number of the iteration. It shows our method enjoys a good robustness performance when the packet dropouts occur.

TABLE VII
ROBUST PERFORMANCE FOR THE THREE TEST SYSTEMS

Probability/ ρ_E	Number of Iterations		
	IEEE 33-bus	Case 69-bus	Case136-bus
0	51	47	35
0.01	62	49	42
0.05	71	65	53
0.1	85	72	121
0.2	122	109	167

VII. CONCLUSION

An event-driven P2P electricity trading market considering network constraints is proposed to support the short-term or immediate local energy transactions in a distribution network. First, the event-driven P2P market framework is briefly outlined in three aspects: market agents, market operation rules, and event-driven rules. Then, the impacts of P2P transactions on the distribution network are quantified by the sensitivity analysis of voltage and loss and network constraints are further included in the market clearing problem. Hence, the endogenous cost of P2P energy trading can be reflected by the LMP as the externality of operational constraints is internalized in the market clearing process. Moreover, the market is cleared using a generalized fast dual ascent method based on which a negotiation mechanism between the participants and market operator is designed with preserving agents' privacy. The numerical results show the proposed market framework could effectively address the P2P energy transactions without violating the operational constraints of the distribution network, and the employed distributed solution method enjoys good convergence and scalability properties in the three test systems.

APPENDIX

A. Proof of Lemma-1

For ease of description, the problem (31) can be equivalently transformed into a general formulation with equality constraints by introducing the auxiliary variables, i.e., $\mathbf{z}_1$ and $\mathbf{z}_2$:

$$\begin{cases} \min\limits_{\mathbf{p},\mathbf{q}\in\Omega} f(\mathbf{p},\mathbf{q}) := \frac{1}{2}\left\|\mathbf{p}-\mathbf{p}_r\right\|_{\mathbf{H_P}}^2 + \frac{1}{2}\left\|\mathbf{q}-\mathbf{q}_r\right\|_{\mathbf{H_Q}}^2 \\ \mathbf{D}_{\mathrm{P}}^{\mathrm{V}}\mathbf{p} + \mathbf{D}_{\mathrm{Q}}^{\mathrm{V}}\mathbf{q} + diag(\mathbf{z}_1)\mathbf{z}_1 = \bar{\mathbf{V}} \quad \boldsymbol{\mu}_{\max} \\ -\mathbf{D}_{\mathrm{P}}^{\mathrm{V}}\mathbf{p} - \mathbf{D}_{\mathrm{Q}}^{\mathrm{V}}\mathbf{q} + diag(\mathbf{z}_2)\mathbf{z}_2 = \underline{\mathbf{V}}, \boldsymbol{\mu}_{\min} \\ 1_N\mathbf{p} - \mathbf{D}_{\mathrm{P}}^{\mathrm{P}}\mathbf{p} + \mathbf{D}_{\mathrm{Q}}^{\mathrm{P}}\mathbf{q} = 0 \quad \lambda_p \\ 1_N\mathbf{q} + \mathbf{D}_{\mathrm{P}}^{\mathrm{Q}}\mathbf{p} - \mathbf{D}_{\mathrm{Q}}^{\mathrm{Q}}\mathbf{q} = 0 \quad \lambda_q \end{cases} \tag{A1}$$

Then, the dual function can be written as

$$\Pi(\boldsymbol{\delta}) := \inf_{\mathbf{p},\mathbf{q},\mathbf{z}_1,\mathbf{z}_2} \ell = d(\boldsymbol{\delta}) - \psi(\boldsymbol{\delta}) \tag{A2}$$

where $\psi(\boldsymbol{\delta}) = \min\limits_{\mathbf{z}_1,\mathbf{z}_2}(\boldsymbol{\mu}_{\max}^T * diag(\mathbf{z}_1)\mathbf{z}_1 + \boldsymbol{\mu}_{\min}^T * diag(\mathbf{z}_2)\mathbf{z}_2)$.

Define $\boldsymbol{\mu} := [\boldsymbol{\mu}_{\max}, \boldsymbol{\mu}_{\min}]$. Then, we have $\psi(\boldsymbol{\delta}) = \sum_{i=1}^{i=2*N_A}\psi_i(\mu_i)$ and

$$\psi_i(\mu_i) = \begin{cases} 0 & \mu_i \ge 0 \\ +\infty & otherwise \end{cases} \tag{A3}$$

For ease of the follow-up description, we further assumed that the function $\psi_i(\mu_i)$ is a continuous convex function, as shown in fig.5. It is supposed that the values of derivative of $\psi_i(\mu_i)$ are sufficiently small when $\mu_i \le 0$ so that the strong duality of $\Pi(\boldsymbol{\delta})$ is guaranteed.

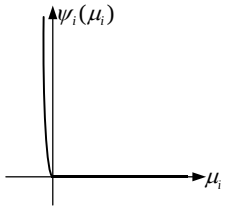

Fig.5 Diagram of the function $\psi_i(\mu_i)$

Define $\boldsymbol{\gamma} := \left[\boldsymbol{\beta}_{\max}^{\mathrm{T}} \quad \boldsymbol{\beta}_{\min}^{\mathrm{T}} \quad \pi_p \quad \pi_q\right]^{\mathrm{T}}$ and the following quadratic approximation of the dual function $\Pi(\boldsymbol{\delta})$ obtains.

$$\varphi_{\mathbf{L}}(\boldsymbol{\delta},\ \boldsymbol{\gamma}) := -d(\boldsymbol{\gamma}) - \left\langle \nabla d(\boldsymbol{\gamma}), \boldsymbol{\delta}-\boldsymbol{\gamma}\right\rangle + \frac{1}{2}\left\|\boldsymbol{\delta}-\boldsymbol{\gamma}\right\|_{\mathbf{L}}^2 + \psi(\boldsymbol{\delta}) \tag{A4}$$

Define

$$\boldsymbol{\delta}'(\boldsymbol{\gamma}) := \arg\min_{\boldsymbol{\delta}}(\varphi_{\mathbf{L}}) \tag{A5}$$

Then, the following corollary can be obtained.

(Corollary 1) Assuming that $\mathbf{L} \succeq \mathbf{M}\mathbf{H}^{-1}\mathbf{M}^T$ then for any $\boldsymbol{\delta}$, we have

$$-\Pi(\boldsymbol{\delta}) + \Pi(\boldsymbol{\delta}') \ge \frac{1}{2}\left\|\boldsymbol{\delta}'-\boldsymbol{\gamma}\right\|_{\mathbf{L}}^2 + \left\langle \boldsymbol{\gamma}-\boldsymbol{\delta}, \mathbf{L}(\boldsymbol{\delta}'-\boldsymbol{\gamma})\right\rangle \tag{A6}$$

Proof. From (33), we have

$$-\Pi(\boldsymbol{\delta}) \le \varphi_{\mathbf{L}}(\boldsymbol{\delta},\ \boldsymbol{\gamma}) \tag{A7}$$

Thus, it yields,

$$-\Pi(\boldsymbol{\delta}) + \Pi(\boldsymbol{\delta}') \ge -\Pi(\boldsymbol{\delta}) - \varphi_{\mathbf{L}}(\boldsymbol{\delta}', \boldsymbol{\gamma}) \tag{A8}$$

Since the functions -*d* and $\psi(\boldsymbol{\delta})$ are both convex, it gets

$$-d(\boldsymbol{\delta}) \ge -d(\boldsymbol{\gamma}) + \left\langle \boldsymbol{\delta}-\boldsymbol{\gamma}, -\nabla d(\boldsymbol{\gamma})\right\rangle \tag{A9}$$

$$\psi(\boldsymbol{\delta}) \ge \psi(\boldsymbol{\delta}') + \left\langle \boldsymbol{\delta}-\boldsymbol{\delta}', \nabla\psi(\boldsymbol{\delta}')\right\rangle \tag{A10}$$

Substituting (A9) and (A10) into (A8) yields

$$\begin{aligned} -\Pi(\boldsymbol{\delta}) + \Pi(\boldsymbol{\delta}') &\ge -d(\boldsymbol{\gamma}) + \left\langle \boldsymbol{\delta}-\boldsymbol{\gamma}, -\nabla d(\boldsymbol{\gamma})\right\rangle + \psi(\boldsymbol{\delta}') \\ &\quad + \left\langle \boldsymbol{\delta}-\boldsymbol{\delta}', \nabla\psi(\boldsymbol{\delta}')\right\rangle - \varphi_{\mathbf{L}}(\boldsymbol{\delta}',\ \boldsymbol{\gamma}) \\ &= \left\langle \boldsymbol{\delta}-\boldsymbol{\gamma}, -\nabla d(\boldsymbol{\gamma})\right\rangle + \left\langle \boldsymbol{\delta}-\boldsymbol{\delta}', \nabla\psi(\boldsymbol{\delta}')\right\rangle + \\ &\quad \left\langle \nabla d(\boldsymbol{\gamma}), \boldsymbol{\delta}'-\boldsymbol{\gamma}\right\rangle - \frac{1}{2}\left\|\boldsymbol{\delta}'-\boldsymbol{\gamma}\right\|_{\mathbf{L}}^2 \\ &= \left\langle \boldsymbol{\delta}-\boldsymbol{\delta}', -\nabla d(\boldsymbol{\gamma}) + \nabla\psi(\boldsymbol{\delta}')\right\rangle - \frac{1}{2}\left\|\boldsymbol{\delta}'-\boldsymbol{\gamma}\right\|_{\mathbf{L}}^2 \\ &= \left\langle \boldsymbol{\delta}'-\boldsymbol{\delta}, \mathbf{L}(\boldsymbol{\delta}'-\boldsymbol{\gamma})\right\rangle - \frac{1}{2}\left\|\boldsymbol{\delta}'-\boldsymbol{\gamma}\right\|_{\mathbf{L}}^2 \\ &= \frac{1}{2}\left\|\boldsymbol{\delta}'-\boldsymbol{\gamma}\right\|_{\mathbf{L}}^2 + \left\langle \boldsymbol{\gamma}-\boldsymbol{\delta}, \mathbf{L}(\boldsymbol{\delta}'-\boldsymbol{\gamma})\right\rangle \end{aligned} \tag{A11}$$

where in the second equality above we used the first-order optimality conditions of (A5). **The proof is completed.**

As shown in the update rule S2 of algorithm 1, $\boldsymbol{\delta}(t) := \arg\min\limits_{\boldsymbol{\delta}} \varphi_{\mathbf{L}}(\boldsymbol{\delta},\ \boldsymbol{\gamma}(t))$. Then, we apply the Corollary 1 at the points $\{\boldsymbol{\delta} = \boldsymbol{\delta}(t), \boldsymbol{\gamma} = \boldsymbol{\gamma}(t+1)\}$, it yields,

$$\begin{aligned} -\Pi(\boldsymbol{\delta}^{(t)}) + \Pi(\boldsymbol{\delta}^{(t+1)}) &\ge \frac{1}{2}\left\|\boldsymbol{\delta}^{(t+1)}-\boldsymbol{\gamma}^{(t+1)}\right\|_{\mathbf{L}}^2 \\ &\quad + \left\langle \boldsymbol{\gamma}^{(t+1)}-\boldsymbol{\delta}^{(t)}, \mathbf{L}(\boldsymbol{\delta}^{(t+1)}-\boldsymbol{\gamma}^{(t+1)})\right\rangle \end{aligned} \tag{A12}$$

Likewise, at the points $\{\boldsymbol{\delta} = \boldsymbol{\delta}^*, \boldsymbol{\gamma} = \boldsymbol{\gamma}^{(t+1)}\}$, we have

$$\begin{aligned} -\Pi(\boldsymbol{\delta}^*) + \Pi(\boldsymbol{\delta}^{(t+1)}) &\ge \frac{1}{2}\left\|\boldsymbol{\delta}^{(t+1)}-\boldsymbol{\gamma}^{(t+1)}\right\|_{\mathbf{L}}^2 \\ &\quad + \left\langle \boldsymbol{\gamma}^{(t+1)}-\boldsymbol{\delta}^*, \mathbf{L}(\boldsymbol{\delta}^{(t+1)}-\boldsymbol{\gamma}^{(t+1)})\right\rangle \end{aligned} \tag{A13}$$

The dual function at the t^{th} iteration and the optimum are respectively abbreviated as $\Pi^{(t)}$ and Π^* hereafter except noted. Multiply the inequality (A12) by $(\sigma^{(t+1)}-1)$ and then add it to the inequality (A13), it yields

$$\begin{aligned} &(\sigma^{(t+1)}-1)(-\Pi^{(t)} + \Pi^*) - \sigma^{(t+1)}(-\Pi^{(t+1)} + \Pi^*) \\ &\ge \frac{\sigma^{(t+1)}}{2}\left\|\boldsymbol{\delta}^{(t+1)}-\boldsymbol{\gamma}^{(t+1)}\right\|_{\mathbf{L}}^2 + \\ &\quad \left\langle \sigma^{(t+1)}\boldsymbol{\gamma}^{(t+1)} - (\sigma^{(t+1)}-1)\boldsymbol{\delta}^{(t)} - \boldsymbol{\delta}^*, \mathbf{L}(\boldsymbol{\delta}^{(t+1)}-\boldsymbol{\gamma}^{(t+1)})\right\rangle \end{aligned} \tag{A13}$$

Multiplying the inequality (A13) by $\sigma^{(t+1)}$ and using the update rule in S3, we obtain

$$\begin{aligned} &2(\sigma^{2(t)})(-\Pi^{(t)} + \Pi^*) - 2\sigma^{2(t+1)}(-\Pi^{(t+1)} + \Pi^*) \\ &\ge \left\|\sigma^{(t+1)}(\boldsymbol{\delta}^{(t+1)}-\boldsymbol{\gamma}^{(t+1)})\right\|_{\mathbf{L}}^2 + \\ &\quad 2\sigma^{(t+1)}\left\langle \sigma^{(t+1)}\boldsymbol{\gamma}^{(t+1)} - (\sigma^{(t+1)}-1)\boldsymbol{\delta}^{(t)} - \boldsymbol{\delta}^*, \mathbf{L}(\boldsymbol{\delta}^{(t+1)}-\boldsymbol{\gamma}^{(t+1)})\right\rangle \\ &= \left\|\sigma^{(t+1)}\boldsymbol{\delta}^{(t+1)} - (\sigma^{(t+1)}-1)\boldsymbol{\delta}^{(t)} - \boldsymbol{\delta}^*\right\|_{\mathbf{L}}^2 - \\ &\quad \left\|\sigma^{(t+1)}\boldsymbol{\gamma}^{(t+1)} - (\sigma^{(t+1)}-1)\boldsymbol{\delta}^{(t)} - \boldsymbol{\delta}^*\right\|_{\mathbf{L}}^2 \\ &= \left\|\sigma^{(t+1)}\boldsymbol{\delta}^{(t+1)} - (\sigma^{(t+1)}-1)\boldsymbol{\delta}^{(t)} - \boldsymbol{\delta}^*\right\|_{\mathbf{L}}^2 - \\ &\quad \left\|(\sigma^{(t)}\boldsymbol{\delta}^{(t)} - (\sigma^{(t)}-1)\boldsymbol{\delta}^{(t-1)} - \boldsymbol{\delta}^*\right\|_{\mathbf{L}}^2 \end{aligned} \tag{A14}$$

where in the first equality the Pythagoras relation is used and in the second equality the update rule in S4 is applied.

Summing over iterations, it yields

$$2\sigma^{2(t)}(-\Pi^{(t)}+\Pi^*) \le 2(\sigma^{2(1)})(-\Pi^{(1)}+\Pi^*) - \left\|\sigma^{(t)}\boldsymbol{\delta}^{(t)}-(\sigma^{(t)}-1)\boldsymbol{\delta}^{(t-1)}-\boldsymbol{\delta}^*\right\|_{\mathbf{L}}^2 - \left\|(\sigma^{(1)}\boldsymbol{\delta}^{(1)}-(\sigma^{(1)}-1)\boldsymbol{\delta}^{(0)}-\boldsymbol{\delta}^*\right\|_{\mathbf{L}}^2$$

$$\le 2(\sigma^{2(1)})(-\Pi^{(1)}+\Pi^*) + \left\|(\sigma^{(1)}\boldsymbol{\delta}^{(1)}-(\sigma^{(1)}-1)\boldsymbol{\delta}^{(0)}-\boldsymbol{\delta}^*\right\|_{\mathbf{L}}^2 \quad \text{(A15)}$$

The sequence $\{\sigma^{(t)}\}$ generated in S4 with $\sigma^{(1)}=1$ satisfies $\sigma^{(t)} \ge (t+1)/2$ for all $t \ge 1$. Thus, we have

$$-\Pi^{(t)}+\Pi^* \le \frac{2}{(t+1)^2}[2(\sigma^{2(1)})(-\Pi^{(1)}+\Pi^*) + \left\|(\sigma^{(1)}\boldsymbol{\delta}^{(1)}-(\sigma^{(1)}-1)\boldsymbol{\delta}^{(0)}-\boldsymbol{\delta}^*\right\|_{\mathbf{L}}^2]$$

$$\le \frac{2}{(t+1)^2}[2\left\langle \boldsymbol{\delta}^*-\boldsymbol{\gamma}^{(1)}, \mathbf{L}(\boldsymbol{\delta}^{(1)}-\boldsymbol{\gamma}^{(1)})\right\rangle + \left\|(\boldsymbol{\delta}^{(1)}-\boldsymbol{\delta}^*\right\|_{\mathbf{L}}^2 - \left\|\boldsymbol{\delta}^{(1)}-\boldsymbol{\gamma}^{(1)}\right\|_{\mathbf{L}}^2]$$

$$= \frac{2\left\|\boldsymbol{\delta}^*-\boldsymbol{\gamma}^{(1)}\right\|_{\mathbf{L}}^2}{(t+1)^2} \quad \text{(A16)}$$

where Corollary 1 is applied at the points ($\boldsymbol{\delta} := \boldsymbol{\delta}^*, \boldsymbol{\gamma} := \boldsymbol{\gamma}^{(1)}$) in the second inequality. Define $\boldsymbol{\gamma}^{(1)} = \boldsymbol{\delta}^{(0)}$, the desired result follows.

REFERENCES

[1] E. Mengelkamp, J. Gärttner, K. Rock, S. Kessler, L. Orsini, and C. Weinhardt, "Designing microgrid energy markets: A case study: The Brooklyn microgrid," *Appl. Energy*, vol. 210, pp. 870–880, Jan. 2018.

[2] Piclo, "Building software for a smarter energy future", 2019, [Online]. Available: https://piclo.energy.

[3] C. Feng, F. Wen, S. You, Z. Li, "Coalitional game-based transactive energy management in local energy communities," *IEEE Trans. Power Syst.*, vol. 35, no. 3, pp. 1729-1740, May 2020.

[4] J. Kim, Y. Dvorkin, "A P2P-dominant distribution system architecture," *IEEE Trans. Power Syst.*, vol. 35, no. 4, pp. 2716- 2725, Jul. 2020.

[5] J. Guerrero, A. C. Chapman. G. Verbic, "Decentralized P2P energy trading under network constraints in a low-voltage network," *IEEE Trans. Smart Grid*, vol. 10, no. 5, pp. 5163-5173, Sept. 2019.

[6] M. K. Alashery, Z. Yi, D. Shi, et al., "A Blockchain-enabled multi-settlement quasi-ideal peer-to-peer trading framework," *IEEE Trans. Smart Grid*, vol. 12, no. 1, pp. 885-896, Jan. 2021.

[7] K. Chen, J. Lin, and Y. Song, "Trading strategy optimization for a prosumer in continuous double auction-based peer-to-peer market: A prediction-integration model," *Appl. Energy*, vol. 242, pp. 1121–1133, May 2019.

[8] S. Park, J. Lee, S. Bae, G. Hwang and J. K. Choi, "Contribution-based energy-trading mechanism in microgrids for future smart grid: a game theoretic approach," *IEEE Transactions on Industrial Electronics*, vol. 63, no. 7, pp. 4255-4265, July 2016.

[9] J. Li, C. Zhang, Z. Xu, J. Wang, J. Zhao, et al., "Distributed transactive energy trading framework in distribution networks," *IEEE Trans. Power Syst*., vol. 33, no. 6, pp. 7215-7227, Nov. 2018.

[10] H. Kim, J. Lee, S. Bahrami, and V. Wong, "Direct energy trading of microgrids in distribution energy market," *IEEE Trans. Power Syst*., vol. 35, no. 1, pp. 639-651, Jan. 2020.

[11] T. Morstyn, A. Teytelboym, and M. D. Mcculloch, "Bilateral contract networks for peer-to-peer energy trading," *IEEE Trans. Smart Grid*, vol. 10, no. 2, pp. 2026–2035, Mar. 2019.

[12] W. Lee, L. Xiang, R. Schober, and V. W. S. Wong, "Direct electricity trading in smart grid: A coalitional game analysis," *IEEE J. Sel. Areas Commun*., vol. 32, no. 7, pp. 1398–1411, Jul. 2014

[13] F. Luo, Z. Y. Dong, G. Liang, et al., "A distributed electricity trading system in active distribution networks based on multi-agent coalition and blockchain," *IEEE Trans. Power Syst*., vol. 34, no. 5, pp. 4097–4108, Sept. 2019.

[14] A. Paudel, K. Chaudhari, C. Long, et al., "Peer-to-peer energy trading in a smart grid considering power losses and network fees," *IEEE Trans. on Smart Grid*, vol. 11, no. 6, pp. 4727-4737, Nov. 2020.

[15] Z. Guo, P. Pinson, S. Chen, et al., "Online optimization for real-time peer-to-peer electricity market mechanisms," *IEEE Trans. Smart Grid*, vol. 12, no. 5, pp. 4151-4163, Sept. 2021.

[16] T. Chen, W. Su, "Indirect customer-to-customer energy trading with reinforcement learning," *IEEE Trans. Smart Grid*, vol. 10, no. 4, pp. 4338-4348, Jul. 2019.

[17] H. Wang, J. Huang, "Incentivizing energy trading for interconnected microgrids," *IEEE Trans. Smart Grid*, vol. 9, no. 4, pp. 2647-2657, Jul. 2018.

[18] T. Baroche, P. Pinson, R. L. Latimier, H. B. Ahmed, "Exogenous cost allocation in peer-to-peer electricity markets," *IEEE Trans. Power Syst*., vol. 34, no. 4, pp. 2553-2564, Jul. 2019.

[19] X. Yang, G. Wang, H. He, J. Lu, and Y. Zhang, "Automated demand response framework in ELNs: Decentralized scheduling and smart contract," *IEEE Trans. Syst., Man, Cybern., Syst*., vol. 50, no. 1, pp. 58–72, Jan. 2020.

[20] Y. Li and B. Hu, "An iterative two-layer optimization charging and discharging trading scheme for electric vehicle using consortium blockchain," *IEEE Transactions on Smart Grid*, vol. 11, no. 3, pp. 2627-2637, May 2020.

[21] S.Wang, A. F. Taha, J. Wang, et al., "Energy crowdsourcing and peer-to-peer energy trading in blockchain-enabled smart grids," *IEEE Trans. Syst., Man, Cybernetics: Syst*., vol. 49, no. 8, pp. 1612–1623, Aug. 2019.

[22] Sun, X. Wu, J. Wang, D. Hou, and S. Wang, "Power compensation of network losses in a microgrid with BESS by distributed consensus algorithm," *IEEE Trans. on Systems, Man, and Cybernetics: Systems*, vol. 51, no. 4, pp. 2091-2100, 2021.

[23] A. J. Conejo and J. A. Aguado, "Multi-area coordinated decentralized DC optimal power flow," *IEEE Trans. Power Syst*, vol. 13, no. 4, pp. 1272–1278, Nov. 1998

[24] M. Arnold, S. Knopfli, and G. Andersson, "Improvement of OPF decomposition methods applied to multi-area power systems," *Proc. Power Tech*, Lausanne, Switzerland, Jul. 1–5, 2007.

[25] C. Feng, Z. Li, M. Shahidehpour, F. Wen, et al., "Decentralized short-term voltage control in active power distribution systems," *IEEE Trans. Smart Grid*, vol. 9, no. 5, pp. 4566–4576, Sep. 2018.

[26] A. Kargarian and Y. Fu, "System of systems-based security-constrained unit commitment incorporating active distribution grids," *IEEE Trans. Power Syst*, vol. 29, no. 5, pp. 2489–2498, Sep. 2014.

[27] D. P. Bertsekas, Nonlinear Programming, 3rd ed. Belmont, MA, USA: Athena Scientific, 2016.

[28] Y. Nesterov, "Smooth minimization of non-smooth functions," *Math. Program*., vol. 103, no. 1, pp. 127-152, May 2005.

[29] A. Beck and M. Teboulle, "A fast iterative shrinkage-thresholding algorithm for linear inverse problems," *SIAM J. Imag. Sci*., vol. 2, no. 1, pp. 183–202, Mar. 2009.

[30] P. Giselsson, "Improved dual decomposition for distributed model predictive control," *IFAC Proc*., vol. 47, no. 3, pp. 1203–1209, Aug. 2014.

[31] Y. Guo, H. Gao, Z. Wang, "Distributed online voltage control for wind farms using generalized fast dual ascent," *IEEE Trans. Power Syst.*, vol. 35, no. 6, pp. 4505-4516, Nov. 2020.

[32] H. Yuan, F. Li, Y. Wei, et al., "Novel linearized power flow and linearized OPF models for active distribution networks with application in Distribution LMP," *IEEE Trans. Smart Grid*, vol. 9, no. 1, pp. 438-448, Jan. 2018.

[33] J. Yang, Z. Dong, F. Wen, et al., "Spot electricity market design for a power system characterized by high penetration of renewable energy generation," *IET Energy Conversion and Economics*, vol. 2, no. 2, pp. 67-78, May 2021.

[34] L. Bai, J. Wang, C. Wang, C. Chen and F. Li, "Distribution locational marginal pricing (DLMP) for congestion management and voltage support," *IEEE Trans. Power Syst*., vol. 33, no. 4, pp. 4061-4073, July 2018.

[35] G. Hasslinger, O. Hohlfeld, "The Gilbert-Elliott model for packet loss in real time services on the Internet," in *Proc. 14th GI/ITG Conf. MMB*, 2008, pp. 1–15.

[36] J. Zhang, S. Nabavi, A. Chakrabortty, Y. Xin, "ADMM optimization strategies for wide-area oscillation monitoring in power systems under asynchronous communication delays," *IEEE Trans. Smart Grid*, vol. 7, no. 4, pp. 2123-2133, Jul. 2016.

[37] A. Yogarathinam, N. R. Chaudhuri, "Wide-area damping control using multiple DFIG-based wind farms under stochastic data packet dropouts," *IEEE Trans. Smart Grid*, vol. 9, no. 4, pp. 3383-3393, Jul. 2018.

Changsen Feng received the B.E. degree in electrical engineering from Shandong University, Jinan, China, in 2013, and the Ph.D. degree from Zhejiang University, Hangzhou, China, in 2019. He joined the Faculty of Zhejiang University of Technology in July 2019 and is currently an Assistant Professor with the College of Information Engineering. His research interests include game theory, machine learning, and optimization theory in power systems.

Bomiao Liang (Member, IEEE) received the B.S. and Ph.D. degrees in electrical engineering from Zhejiang University, Hangzhou, China, in 2012 and 2017, respectively. She was on practicum exchange with UNSW Business School, University of New South Wales, from 2015 to 2016. She is currently a Lecturer with the School of Automation and Electrical Engineering, Zhejiang University of Science and Technology, Hangzhou, China. Her research interests include transactive energy, integrated energy systems, and smart grid.

Zhengmao Li (Member, IEEE) received the B.E. degree in information engineering and the M.E. degree in electrical engineering from Shandong University, Jinan, China, in 2013 and 2016, respectively, and the Ph.D. degree in electrical engineering

from the School of Electrical and Electronic Engineering, Nanyang Technological University, Singapore, in 2020. During 2019-2021, he was a Research Fellow with the Stevens Institute of Technology, Hoboken, NJ, USA, and he is currently a Research Fellow with Nanyang Technological University. His research interests include renewable energy integration, microgrid and multi-energy system, and optimization techniques such as approximate dynamic programming, robust optimization, and stochastic optimization.

Weijia Liu (Member, IEEE) received the B.Eng. and Ph.D. degrees in electrical engineering from Zhejiang University, Hangzhou, China, in 2011 and 2016, respectively. He is currently a Researcher with Power System Engineering Center, National Renewable Energy Laboratory. His research interests include power system restoration and resilience, integrated energy systems, and smart grid.

Fushuan Wen (Fellow, IEEE) has been a full professor in *Zhejiang University*, China since 1997. He is also a part-time distinguished professor in *Hangzhou Dianzi University*, China, a part-time professor in *Tallinn University of Technology*, Estonia, and a visiting principal research scientist in *Shenzhen Institute of Artificial Intelligence and Robotics for Society*, China. He has been listed in "Most Cited Chinese Researchers" in six consecutive years since 2015 by Elsevier. He is the Editor-in-Chief of *Energy Conversion and Economics* (IET), the deputy Editor-in-Chief of *Automation of Electric Power Systems*, and serves as the editor, subject editor and associate editor of several international journals. His research interests include power industry restructuring, power system alarm processing, fault diagnosis and restoration strategies, smart grids and electric vehicles, as well as artificial intelligence applications in power and integrated energy systems.